PUBLICATIONS of the EARTH PHYSICS BRANCH

VOLUME 41 - NO. 5

a solid-state electrical recording magnetometer

D. F. TRIGG, P. H. SERSON AND P. A. CAMFIELD

DEPARTMENT OF ENERGY, MINES AND RESOURCES

OTTAWA, CANADA 1971

Cat. No.: M70-41/5

Contents

Figure 1. The solid-state, 3 component magnetometer.

a solid-state electrical recording magnetometer

D. F. TRIGG, P. H. SERSON AND P. A. CAMFIELD

Abstract. A solid-state, three-axis recording magnetometer using fluxgate-type magnetic detectors is described. Design theory, circuit details, performance data and operating instructions are provided. Instrument specifications include an output sensitivity of 1 volt per 100 gammas, a -3 db gain roll-off at 3.5 Hz and less than 4 watts power consumption. A comparison of instrument performance when using tuned magnetic detectors with performance when using untuned detectors indicates the superiority of the latter mode of operation.

Résumé. Nous donnons la description d'un magnétomètre enregistreur entièrement transistorisé dont les trois sondes magnétiques placées orthogonalement sont des solénoides à noyau saturable. La théorie, la construction, l'opération et le rendement sont donnés en détail. Les spécifications de l'instrument comprennent une sensibilité de rendement de 1 volt par 100 gammas, un niveau de -3 db à 3.5 Hz et une consommation de puissance de moins que 4 watts. Une comparaison de rendement entre instruments employant des sondes magnétiques syntonisées ou non-syntonisées démontre la supériorité de la dernière méthode d'opération.

Introduction

Three-axis recording magnetometers using fluxgate-type magnetic detectors were used extensively in Canada starting with the International Geophysical Year in 1957. Although these units were intended to be used chiefly at magnetic observatories, applications soon arose in which these magnetometers were transported frequently during research programs, often to inaccessible locations having no indigenous power source. With these problems of transportation and power in mind, the staff of the Geomagnetic Division proceeded to design a solid-state counterpart of the original electrical recording magnetometer described by Serson (1957). The result was the portable, solid-state magnetometer which appears in Figure 1 and is described in detail in the accompanying text. The magnetic detectors now in use are identical with those detailed by Serson (1957), and the magnetometer output is still in the form of three analog voltages proportional to three orthogonal components of magnetic field at a scale of 1 volt per 100 gammas.

Part I of this paper deals with general design information and data and Part II provides all detail necessary to those who must operate and test these instruments.

Part I – Theory of operation

The theory of operation of the magnetometer has been presented by Serson (1957) in a time-domain analysis. A similar analysis in the frequency domain leads rather naturally to analytic expressions for magnetometer response as a function of frequency, and will be presented here for the sake of completeness and continuity of the discussion.

A block diagram of one channel of the magnetometer currently in use by the Earth Physics Branch appears in Figure 2. The oscillator, frequency doubler and tuned amplifier characteristics do not enter directly into the calculations of system response, and are shown only for completeness. The oscillator amplitude will determine the second-harmonic signal voltage available from the fluxgate secondary coil, per Oersted of input magnetic field (Serson and Hannaford, 1956; Primdahl, 1970). A second-harmonic reference signal of sufficient amplitude and purity to ensure proper operation of the phase-sensitive detector is all that is required of the doubler and tuned amplifier. The output of the fluxgate is a second-harmonic signal e_5, proportional to the total axial magnetic field H_T, which is the sum of the earth's ambient magnetic field H_a and the magnetic fields H_f and H_b produced in the fluxgate secondary coil. H_f is generated by the system feedback current I_f, and H_b is the result of bias current I_b. The phase-sensitive detector output e_1 is a d.c. voltage proportional to the amplified fluxgate signal e_6, which is an a.c. voltage. The output of the low-pass filter consisting of R_2 and C_2 is the d.c. voltage e_2, which is integrated to produce the system output voltage e_3. It is assumed in the analysis that the integrator does not load the low-pass filter.

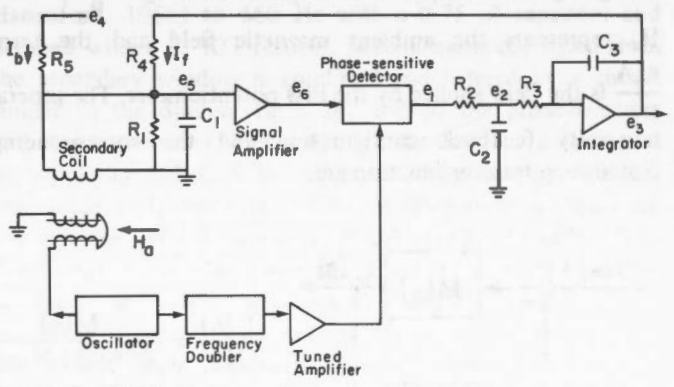

Figure 2. Block diagram of one channel of the magnetometer.

The transfer function F(s) of each element of the block diagram in Figure 2 can be obtained by the methods of control theory (Harrison and Bollinger, 1963). In particular, the transfer function of an element is defined as the ratio of the Laplace transform of the output to the Laplace transform of the input with the assumption that all initial conditions are zero. Listed below are the transfer functions of each element of Figure 2:

1. Fluxgate output: $e_5(s)/H_T(s) = G_1$
2. Fluxgate solenoid: $[H_f(s)+H_b(s)]/[I_f(s)+I_b(s)] = A$
3. Fluxgate signal amplifier: $e_6(s)/e_5(s) = G_2$
4. Phase-sensitive detector: $e_1(s)/e_6(s) = G_3$
5. Low-pass filter: $e_2(s)/e_1(s) = [1/R_2C_2][1/(s+1/R_2C_2)]$
6. Integrator: $e_3(s)/e_2(s) = 1/R_3C_3s$
7. Feedback resistor R_4: $I_f(s)/e_3(s) = 1/R_4$
8. Bias resistor R_5: $I_b(s)/e_4(s) = 1/R_5$

If the reference signal and e_6 are exactly in phase, $G_3=1$. For any other phase relationship $G_3<1$, and at 90° phase difference $G_3=0$.

A block diagram of these transfer functions appears in Figure 3. This diagram can be simplified to the form of Figure 4 by repeated application of the following rules:

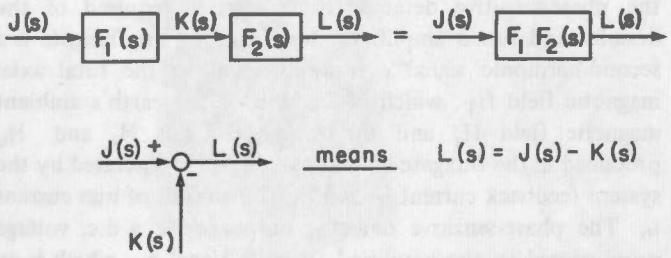

The block diagram of Figure 4 represents the magnetometer as a non-unity feedback system in which the output is the d.c. voltage e_3 and the input is the magnetic field $H_a - \frac{e_4A}{R_5}$, where H_a represents the ambient magnetic field and the term $\frac{e_4A}{R_5}$ is the field applied by the bias potentiometer. The general non-unity feedback configuration and the corresponding closed-loop transfer function are:

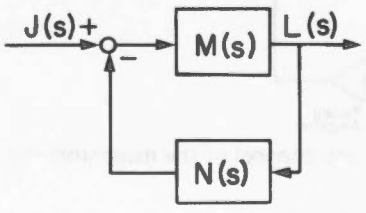

$$\frac{L(s)}{J(s)} = \frac{M(s)}{1+M(s)\,N(s)}$$

Applying this rule to the magnetometer system of Figure 4 gives:

$$\frac{e_3(s)}{H_a(s)-\frac{e_4(s)A}{R_5}} = \frac{\frac{G_1G_2G_3}{R_2C_2R_3C_3(s^2+s/R_2C_2)}}{\frac{G_1G_2G_3}{R_2C_2R_3C_3(s^2+s/R_2C_2)}\cdot\frac{A}{R_4}+1}$$

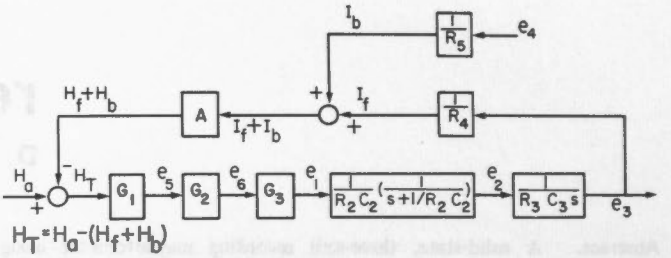

Figure 3. Transfer function block diagram, one channel.

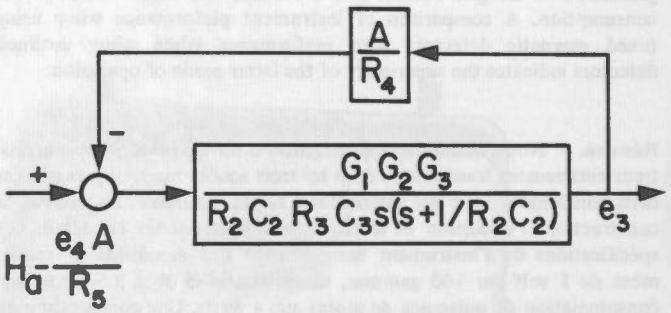

Figure 4. Simplified block diagram, one channel.

which reduces to:

$$\frac{R_2C_2R_3C_3R_4}{G_1G_2G_3A}s^2e_3(s) + \frac{R_3C_3R_4}{G_1G_2G_3A}se_3(s) + e_3(s) = \frac{R_4}{A}H_a(s) - \frac{R_4}{R_5}e_4(s) \quad \ldots\ldots(1)$$

The inverse Laplace transform of equation (1) gives the system differential equation in familiar form:

$$\frac{R_2C_2R_3C_3R_4}{G_1G_2G_3A}\ddot{e}_3 + \frac{R_3C_3R_4}{G_1G_2G_3A}\dot{e}_3 + e_3 = \frac{R_4}{A}H_a - \frac{R_4}{R_5}e_4 \quad \ldots\ldots(2)$$

By comparison of equation (1) with the general second order equation $\frac{s^2f}{\omega_n^2} + \frac{2\delta}{\omega_n}sf + f = K$, in which ω_n is natural frequency and δ is damping ratio, it is seen that for the magnetometer of Figure 2,

$$\omega_n^2 = \frac{G_1G_2G_3A}{R_2C_2R_3C_3R_4} \quad \text{and} \quad \delta^2 = \frac{R_3C_3R_4}{4R_2C_2G_1G_2G_3A}$$

The output sensitivity of the instrument is determined by letting all derivative terms of equation (2) equal zero (steady-state conditions) and assuming the bias field to be constant. In this case $e_3 = \frac{R_4}{A} H_a$, or output sensitivity $\frac{e_3}{H_a} = \frac{R_4}{A}$ volts/oersted. The values actually used for these constants are R_4 = 340,000 ohms and A = 340 oersted/amp., giving a magnetometer output of 1 volt per 100 gammas.

Frequency response

An analytical method for obtaining the magnitude $M(\omega) = \frac{\text{output } O(\omega)}{\text{input } I(\omega)}$ and the phase difference $\phi(\omega)$ between input and output is given in Appendix A. The result of these calculations is:

$$M(\omega) = \frac{R_4}{A}\left[\left(\frac{\omega}{\omega_n}\right)^4 + (4\delta^2 - 2)\left(\frac{\omega}{\omega_n}\right)^2 + 1\right]^{-\frac{1}{2}}$$

$$\phi(\omega) = \cos^{-1}\left\{\left[1 - \left(\frac{\omega}{\omega_n}\right)^2\right]\left[\left(\frac{\omega}{\omega_n}\right)^4 + (4\delta^2 - 2)\left(\frac{\omega}{\omega_n}\right)^2 + 1\right]^{-\frac{1}{2}}\right\}$$

Constants appropriate to the present magnetometers are:

$G_1 = 4\frac{v}{oe}$ (tuned fluxgate) $G_2 = 25$ $G_3 = 1$

$R_4 = 340K\Omega$ $A = 340\frac{oe}{amp}$ $R_2 = 33\,K\Omega$

$C_2 = 1.0\,\mu f$ $R_3 = 120K\Omega$ $C_3 = 0.05\mu f$

and these values result in $f_n = \frac{\omega_n}{2\pi} = 3.5$ Hz and $\delta = 0.67$.

Figure 5 shows M (f) and ϕ (f) plotted against f for a system with the constants given above. It should be noted that changing the value of any component used in calculation of ω_n and δ can alter the magnetometer constants greatly, and will lead to instability if δ approaches 0.

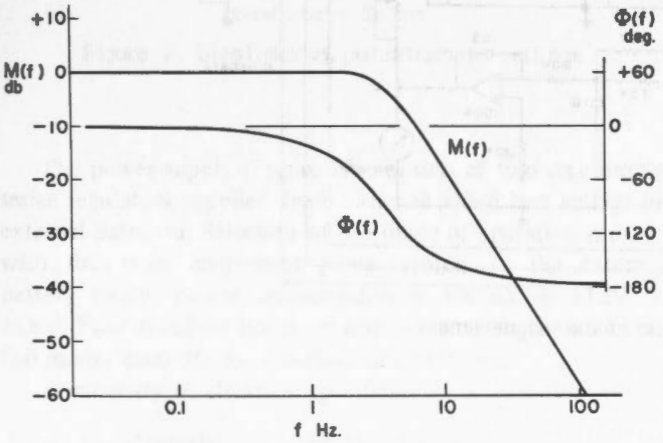

Figure 5. Theoretical frequency response.

Circuit details

A schematic of the 3-component magnetometer currently in use at the Earth Physics Branch appears in Figure 6. The three fluxgates are orthogonally mounted in a sensing head assembly, which also contains a platinum resistance thermometer. The sensing head is connected to the electronics package by means of a multi-conductor cable of any desired length up to several thousand feet.

Excitation current of approximately 100 mA rms is required by the fluxgates and is derived from a Wien-bridge oscillator circuit operating at 330±20Hz. A power booster is included within the oscillator feedback loop to provide the necessary current drive capability. The oscillator amplitude, and hence fluxgate drive current, may be varied by means of the 10KΩ potentiometer. It is of utmost importance that the second-harmonic content (660 Hz) of the drive circuit be minimized. Measured amplitudes at the output of this oscillator circuit are typically 70 db below the fundamental amplitude. Recent work by Primdahl (1970) has shown that a blocking capacitor in series with the 120KΩ resistor in the oscillator circuit lowers the second harmonic content to more than 80 db below the fundamental.

The oscillator output is full-wave rectified, then amplified and filtered by a band-pass filter tuned to the second harmonic at 660 Hz. This filter is simply an operational amplifier with a twin-T network as the feedback element. The 330KΩ shunt across the twin-T network keeps the filter Q low enough that phase shifts due to any variations of oscillator frequency do not reduce phase-sensitive detector gain enough to impair magnetometer response. The doubler output provides the reference signal at the centre-tap of each phase-sensitive detector transformer.

Each fluxgate secondary winding is tuned (Serson and Hannaford, 1956) to 660 Hz with a 0.75 μf capacitor and damped with a 2.7KΩ resistor. Second-harmonic signal from the secondary winding is amplified and filtered by a circuit similar to the doubler filter and fed to the phase-sensitive detector transformer. The output of the detector, a d.c. signal with polarity and amplitude determined by the direction and magnitude of fluxgate axial field, is integrated and fed back through the 340KΩ resistor (330KΩ plus 20KΩ variable) to the fluxgate secondary winding. This provides the negative feedback, and the magnetometer output is taken at the integrator output. It is a measure of the voltage necessary to provide sufficient feedback current through the 340KΩ resistor to produce a field in the fluxgate secondary winding just sufficient to cancel the ambient axial field at the fluxgate. If the total ambient field were to be cancelled by dynamic feedback (for example, a 60,000γ Z component), a much lower value of R_4 would be necessary, since the output voltage of the operational amplifiers is limited to about 12 volts. This means the output sensitivity R_4/A would be greatly reduced, necessitating a sophisticated recording device with a very large dynamic range (equivalent to 60,000γ) and high resolution (about 1γ). In practice, the bulk of the ambient field is

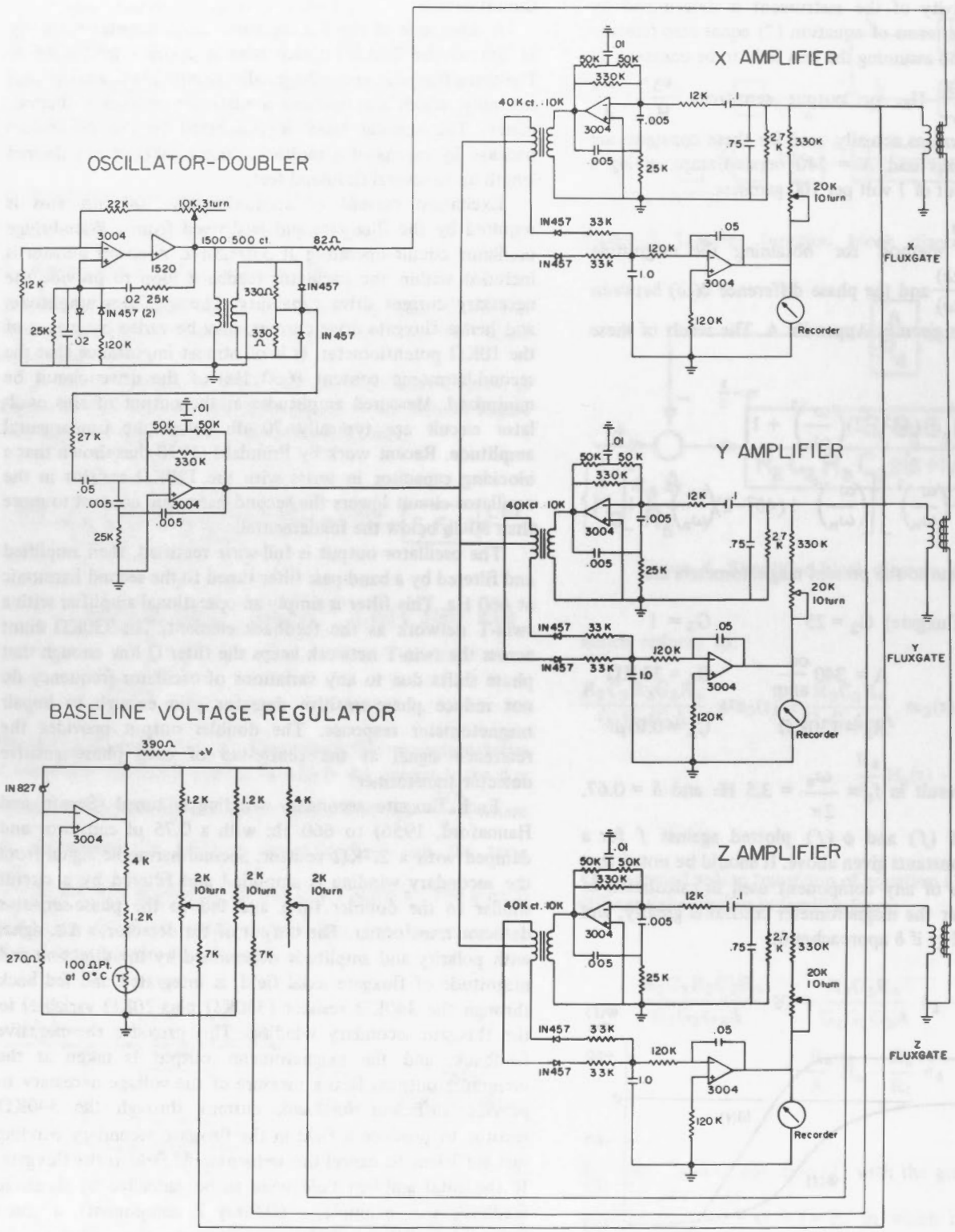

Figure 6. Circuit schematic of the magnetometer.

cancelled by a bias current in the fluxgate secondary, which is obtained from the very stable baseline voltage regulator, and the remainder of the field is then cancelled by dynamic feedback. The baseline voltage is obtained from the 1N827 temperature compensated zener diode (0.001 per cent /° C), which is operated at constant current by the action of the operational amplifier. A platinum resistance thermometer, mounted in the sensing head, provides a bias compensation for the average temperature sensitivity of the fluxgates. Three 10-turn 2KΩ precision potentiometers permit adjustment of the bias current over ranges corresponding to 0 to 20,000 gammas field in the X and Y channels and 46,000 to 67,000 gammas in the Z channel. Curves showing the bias field as a function of potentiometer setting are presented in Figure 7. No attempt has been made to provide baseline controls which are accurately calibrated.

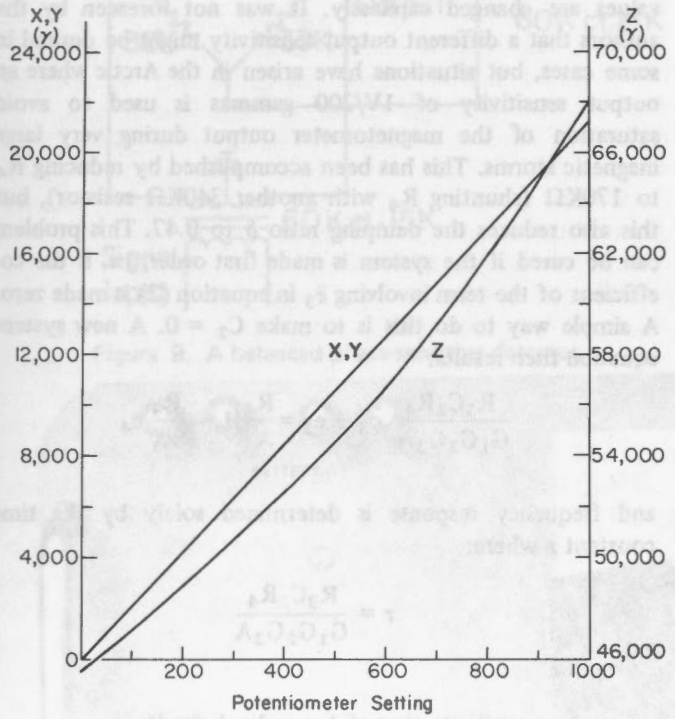

Figure 7. Bias fields vs. potentiometer settings.

The power supply (Figure 13) consists of two very simple series regulators supplied from either rectified line voltage or external batteries. Selection of the mode of operation is made with the main instrument power switch. In the external battery mode, power consumption is ±90mA at ±12V to ±18V. Four hundred hours of operation can be obtained, in this mode, from 40 lbs of carbon-zinc batteries.

A summary of electrical specifications is presented below:

Power requirements:	4W at 115V, 60 Hz or ±90mA at ±12V to ±18V
Baseline adjustment range:	X – 0 to 20,000 gammas Y – 0 to 20,000 gammas Z – 46,000 to 67,000 gammas
Sensitivity:	1V per 100 gammas
Resolution:	1 gamma
Dynamic range:	±1000 gammas (±10V) from baseline
Output impedance:	0Ω
Output current capability:	±20 mA max.
Frequency response:	-3db at 3.5 Hz.

Stability and drift

Data on long-term stability of the magnetometers has been obtained by the Ottawa magnetic observatory and is summarized in the graphs of Figure 8. Here, baseline values for the three components H, D and Z of a magnetometer are plotted against time, starting from January 3, 1969 (day 3) and ending on July 11, 1969 (day 192). The magnetometer and sensing head were located in a thermostatted room. Changes in the Z baseline values are closely correlated with the temperature of the recording room. The thermostat was changed from 22°C to 19°C between days 57 and 66 and on day 177 the temperature rose to 21°C. A temperature coefficient of 10γ per degree explains the main features of the variation in Z. The changes of D baseline are larger than expected (one minute of arc in D corresponds to 4.5γ at Ottawa), and apparently unrelated to temperature. The record from the photographic variometers indicates that the absolute observations of days 57 and 66 are probably in error by 5′. However, no explanation has been found for the fluctuation following day 130.

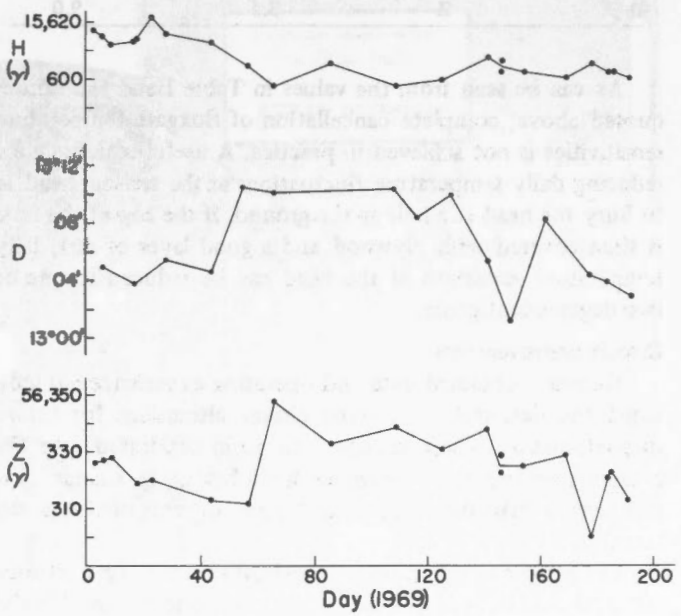

Figure 8. Drifts in component baselines from January 3, 1969 to July 11, 1969.

Tests to determine the temperature sensitivity of fluxgates were carried out by placing sensing heads in a non-magnetic oven and varying the temperature over a range from 20°C to 40°C. The head and oven were in turn mounted within a set of 3-axis Helmholtz coils (Roy *et al.*, 1969), providing an ambient field free of variations. During these tests the thermometer mounted on the sensing head was disabled so that no compensation of thermal drift took place within the magnetometer circuit. Table I presents the drift results for the 3-sensing heads so tested. These drifts are only roughly proportional to the axial field sensed by each fluxgate in the tuned operating mode. The temperature compensation network is designed to provide a change of 56 ppm/°C in bias field on the fluxgates. For the Z component at Ottawa (56,000γ) this provides a compensation of 3γ per °C. Detailed calculations of the temperature compensation network appear in Appendix B.

Table I
Temperature Sensitivity of Fluxgate Sensors

		Untuned gammas/°C	Tuned gammas/°C
Head X 11			
	D	0	1.5
	H	0.5	2.5
	Z	2.5	6.0
Head X 14			
	D	0.2	1.2
	H	0.6	2.5
	Z	3.0	6.0
Head X 26			
	D	0.75	3.0
	H	0.6	7.0
	Z	3.5	9.0

As can be seen from the values in Table I and the figures quoted above, complete cancellation of fluxgate temperature sensitivities is not achieved in practice. A useful technique for reducing daily temperature fluctuations at the sensing head is to bury the head in a hole in the ground. If the top of the hole is then covered with plywood and a good layer of dirt, daily temperature variations at the head can be reduced to one or two degrees centigrade.

Circuit improvements

Recently obtained data and operating experience has indicated the desirability of some circuit alterations for future magnetometers. These changes can be incorporated into the present magnetometer design without having to change anything other than the component layout on some of the circuit boards.

Examination of Table I indicated the first change which should be made. In every case a fluxgate operated in the tuned mode had a higher temperature sensitivity than when it was untuned. Moreover, the drifts in untuned fluxgates are very nearly proportional to the magnetic field sensed by the fluxgate, and the temperature compensation designed into the baseline voltage regulator is nearly sufficient to eliminate these drifts. Certainly a temperature sensitivity less than 1 gamma/°C should be realized in every component. A consequence of removing the tuning capacitance and shunt resistor from the fluxgate secondary circuit is that the fluxgate gain G_1 is reduced, from 4V/0e to 0.75V/0e in the present case. This effect can be compensated (in order to keep ω_n and δ constant) by increasing the a.c. amplifier gain G_2. Since the fluxgate is normally operated with all even harmonics of the output waveform nulled, the amount of fundamental and third harmonic present in the input signal will determine the maximum allowable value for G_2. Care must be taken to ensure that the phase relationship between amplifier output and the reference signal is not severely altered.

A disadvantage of the second order magnetometer system described thus far is that instability can occur if component values are changed carelessly. It was not foreseen by the authors that a different output sensitivity might be desired in some cases, but situations have arisen in the Arctic where an output sensitivity of 1V/200 gammas is used to avoid saturation of the magnetometer output during very large magnetic storms. This has been accomplished by reducing R_4 to 170KΩ (shunting R_4 with another 340KΩ resistor), but this also reduces the damping ratio δ to 0.47. This problem can be cured if the system is made first order, i.e. if the coefficient of the term involving $\ddot{e}_3$ in equation (2) is made zero. A simple way to do this is to make $C_2 = 0$. A new system equation then results:

$$\frac{R_3C_3R_4}{G_1G_2G_3A}\dot{e}_3 + e_3 = \frac{R_4}{A}H_a - \frac{R_4}{R_5}e_4$$

and frequency response is determined solely by the time constant τ where:

$$\tau = \frac{R_3C_3R_4}{G_1G_2G_3A}$$

An analysis similar to that of Appendix A results in:

$$M(\omega) = \frac{R_4}{A}(1 + \omega^2\tau^2)^{-\frac{1}{2}}$$

$$\phi(\omega) = \cos^{-1}(1 + \omega^2\tau^2)^{-\frac{1}{2}}$$

which are the magnitude ratio and phase angle for a first order system.

Since $M(\omega)$ now rolls off at 6 db/octave instead of 12 db/octave the second harmonic content in the magnetometer output will be greater in the first order case (assuming that 1st and 2nd order systems have a similar 3-db roll-off point). The

magnetometer has been designed to be sensitive to second harmonic fluxgate signal so the feedback current must not contain this frequency. To prevent this, either the time constant must be increased, degrading frequency response, or a way must be found to reduce the second harmonic content at the integrator input. The present phase-sensitive detector is not a balanced type, with the result that the whole of the second harmonic reference signal appears at the integrator input when C_2 is removed. A balanced detector of the type shown in Figure 9 eliminates this high second harmonic content.

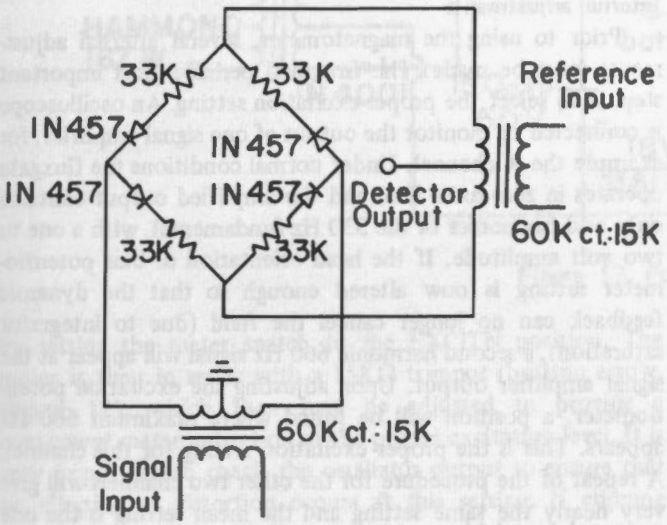

Figure 9. A balanced phase-sensitive detector.

Part II – Magnetometer controls

Figure 10 provides a view of the various magnetometer controls available on the panel. 115V line power enters via the plug mounted just above the fuse holder and alternate battery power may be provided at the four binding posts. The second and third binding posts are wired together internally to provide the electrical ground point. The meter switch has a position labelled OFF which provides a short circuit across the meter terminals, and this should not be confused with the power OFF condition. With the meter switch set at the EXCITN position the meter monitors excitation current, as described later in the Internal Adjustments section. The X, Y and Z switch positions permit the meter to measure the amount and polarity of dynamic feedback applied to the corresponding fluxgate at a scale of 500 gammas–0–500 gammas. B- and B+ switch settings enable the meter to indicate the negative and positive regulated supply voltages respectively. In this case, the numerical meter reading is 20 times the supply voltage, i.e. a meter reading of 240 indicates a regulated supply voltage of 12V. The bias field potentiometers, labelled X, Y and Z and equipped with lockable turns-counting dials, are used in conjunction with the meter switch to bring the magnetometer channels within the range of dynamic feedback operation. Immediately to the right of the 3 bias potentiometers is the excitation current adjustment potentiometer.

Wiring details and power supplies

A schematic of the chassis wiring is presented in Figure 11. The various numbers and letters refer to the labelling of

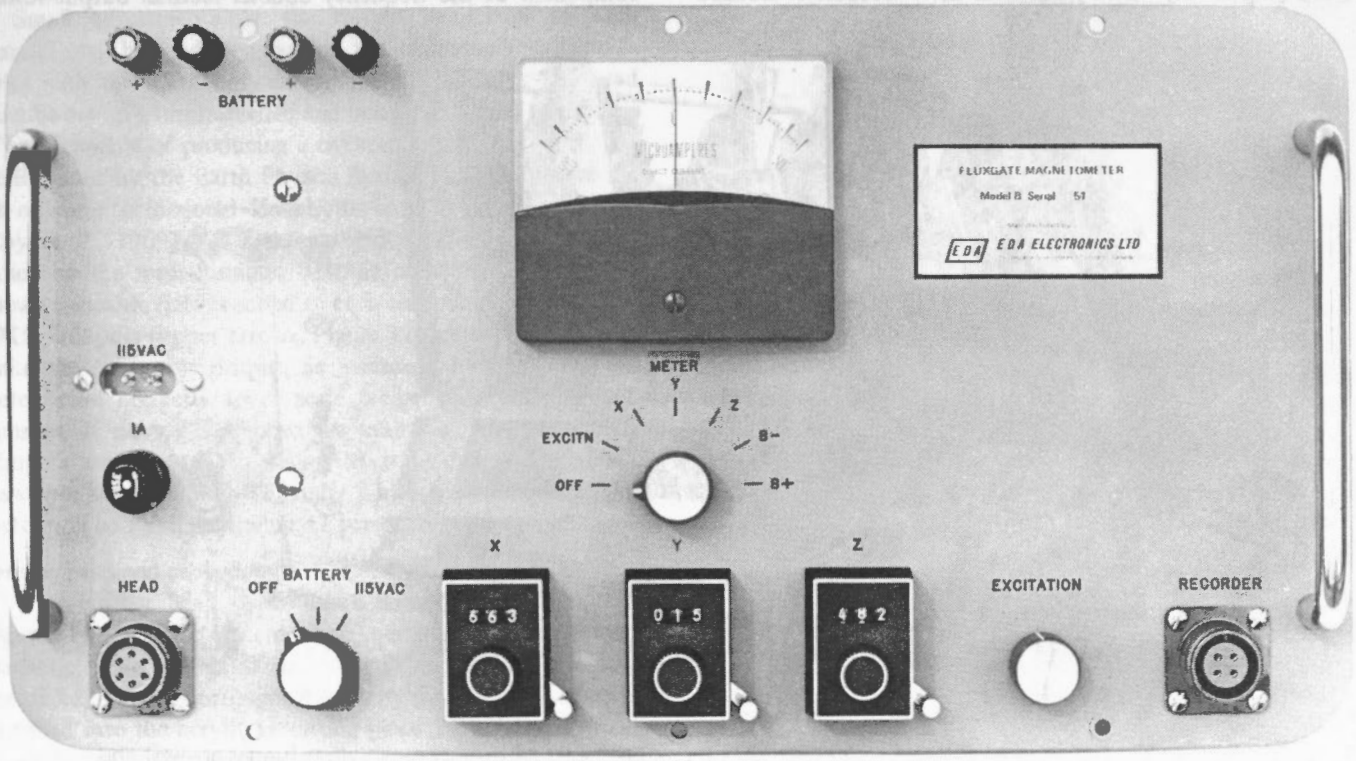

Figure 10. Magnetometer panel controls.

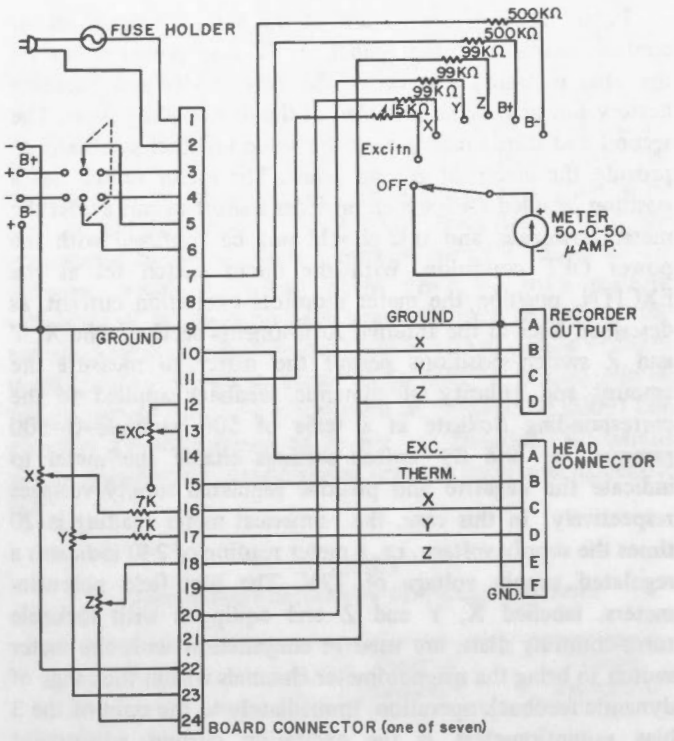

Figure 11. Chassis wiring details.

connector pins and the single 24-pin receptacle indicated in the figure represents seven such receptacles with pins wired in parallel. The electronics has been partitioned to fit on 7 circuit boards (Figure 12) which mate with the 7 receptacles labelled J1 to J7 inclusive (labelling not visible in Figure 12). Each power supply is mounted on a single card and must be mated with either J1 or J2 (right-hand receptacles in Figure 12) for proper operation. The circuits for both power supplies are given in Figure 13. The remaining circuitry partitions into X, Y and Z component amplifier cards, an oscillator-doubler card and a baseline voltage regulator card. These cards may be placed randomly in receptacles J3 to J7 inclusive. No damage will occur if all cards are placed randomly in receptacles but operation is impossible until the power supply cards are placed in J1 and J2.

Internal adjustments

Prior to using the magnetometer, several internal adjustments must be made. The first, and perhaps most important step, is to select the proper excitation setting. An oscilloscope is connected to monitor the output of one signal amplifier, for example the X channel. Under normal conditions the fluxgate operates in zero axial field and the amplified output contains only odd harmonics of the 330 Hz fundamental, with a one to two volt amplitude. If the head orientation or bias potentiometer setting is now altered enough so that the dynamic feedback can no longer cancel the field (due to integrator saturation), a second harmonic 660 Hz signal will appear at the signal amplifier output. Upon adjusting the excitation potentiometer, a position will be found where maximum 660 Hz appears. This is the proper excitation setting for this channel. A repeat of the procedure for the other two channels will give very nearly the same setting and the mean setting is the one desired. The panel meter can be made to sample the d.c. component of the frequency doubler rectifier output voltage

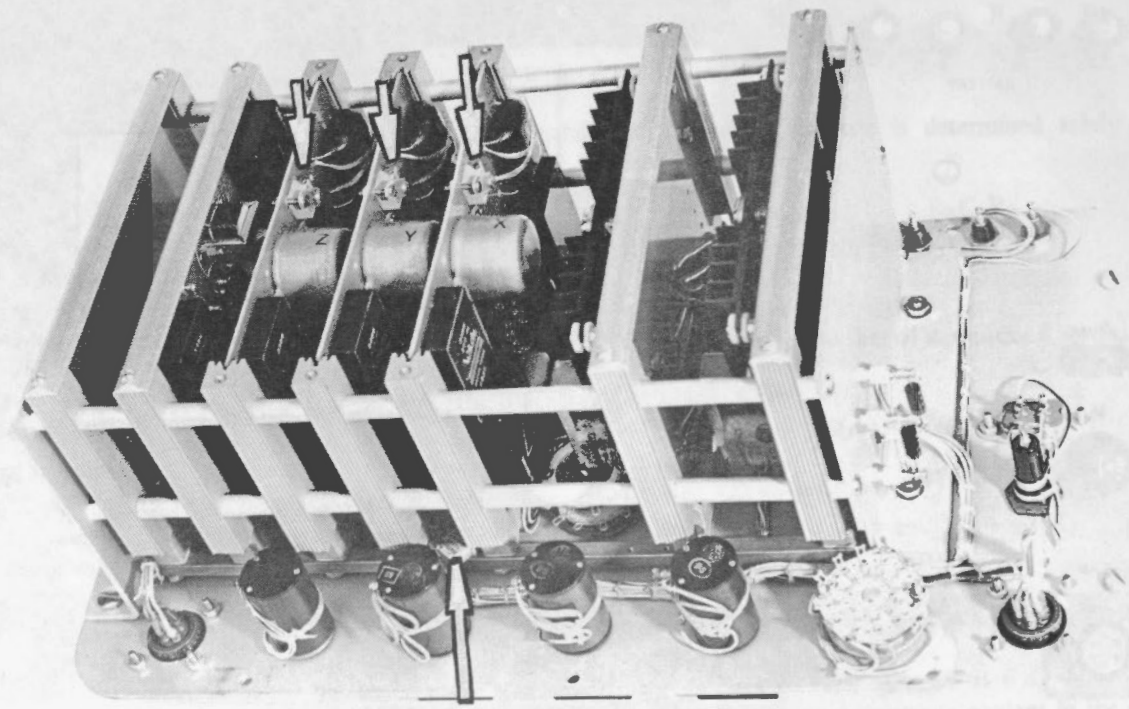

Figure 12. Location of internal potentiometers for adjustments of output sensitivities (upper arrows) and meter reading at desired excitation (lower arrow).

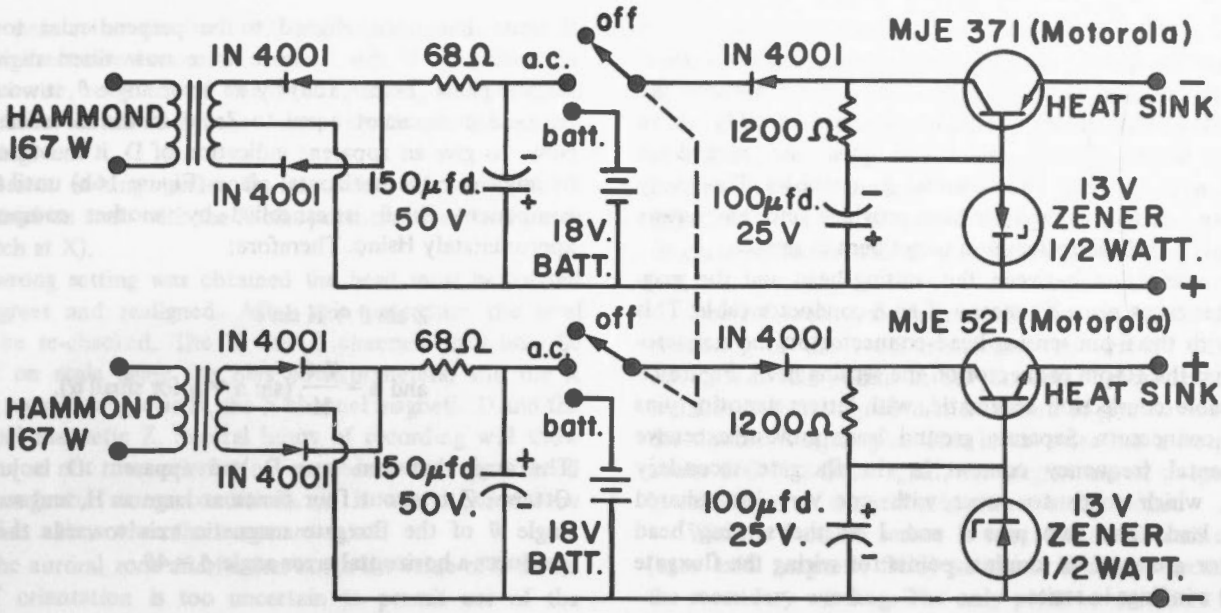

Figure 13. Power supply circuit.

by setting the meter switch to the EXCITN position. The meter is then in series with a 15KΩ trimpot (bottom arrow, Figure 12), which then may be adjusted to provide a convenient meter indication of the proper excitation level. It is very important to check the oscillator output to ensure that no clipping or distortion occurs at this setting. If clipping occurs, the highest excitation setting which produces no clipping should be chosen as the operating point.

Small adjustments of the output sensitivity of each channel may be made by varying the trimming resistance in series with the 330KΩ dynamic feedback resistor. The head must be set up within, levelled and oriented parallel to the axis of coils capable of producing a calibrated magnetic field. The facility used by the Earth Physics Branch for this purpose is a set of three orthogonal Helmholtz coils of 8 feet diameter [Roy *et al.*, 1969]. After the ambient field has been exactly nulled by the magnetometer baseline controls, an accurately known magnetic field is added to each component in turn. The 20KΩ trimpots (upper arrows, Figure 12) are then adjusted to make the integrator output, as measured by a digital voltmeter, read correctly for a scale factor of 1 volt per 100 gammas. If no such facilities are available, the same 20KΩ trimpots are adjusted to make the total dynamic feedback resistance equal to 340KΩ, under which conditions the scale factor will be 1V/100 gammas ±2 per cent.

Sensing head and cable details

The sensing head, with cover removed, is depicted in Figure 14. All components and materials used are non-magnetic. The fluxgates are locked in three accurately-machined, mutually orthogonal holes by means of nylon screws threaded into the acrylic mounting piece. Pliobond rubber adhesive is used to cement the platinum resistance thermometer to the same piece. A graduated circle with 5-degree markings is

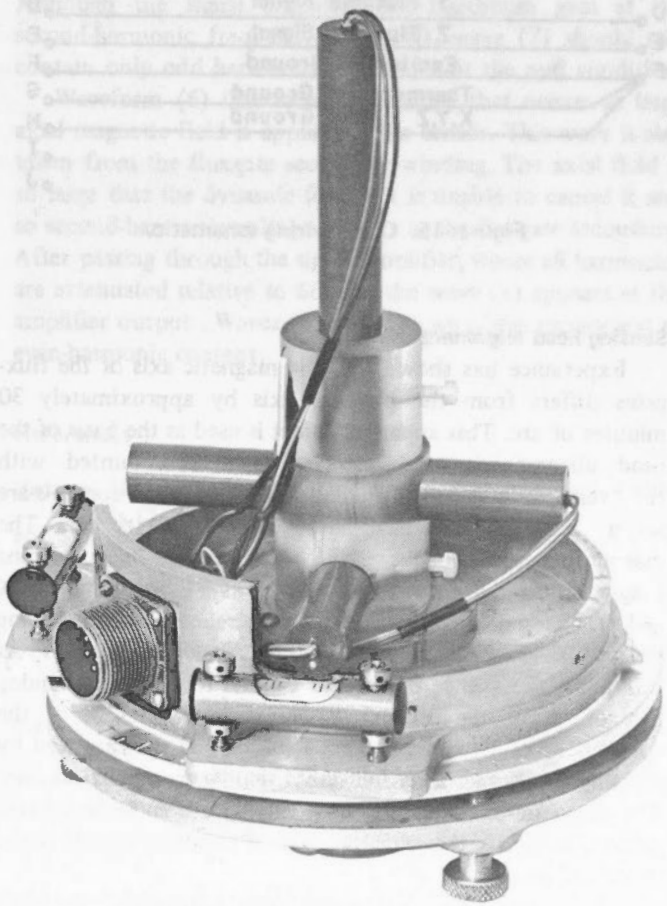

Figure 14. Sensing head with cover removed.

engraved on the baseplate and is useful in the head orientation procedures described later. A teflon gasket ensures smooth differential motion between the engraved baseplate and the upper casting with the pointer. The complete assembly can be mounted on a $1\frac{3}{8}$-inch aluminum pipe and locked in position with two large thumbscrews (not visible). Three very large brass levelling screws have been provided since any screws less than $\frac{3}{8}$-inch diameter seem to get bent in service.

Interconnection between the sensing head and the magnetometer takes place by means of an 8-conductor cable. This mates with the 6-pin sensing head connector on the magnetometer and the 10-pin connector on the sensing head. Figure 15 is the cable connection schematic, with letters denoting pins on the connectors. Separate ground leads prevent excessive fundamental frequency content in the fluxgate secondary circuits, which tends to occur with one very long shared ground lead. The two pins I and J at the sensing head connector are used as terminal points for wiring the fluxgate primary windings in series.

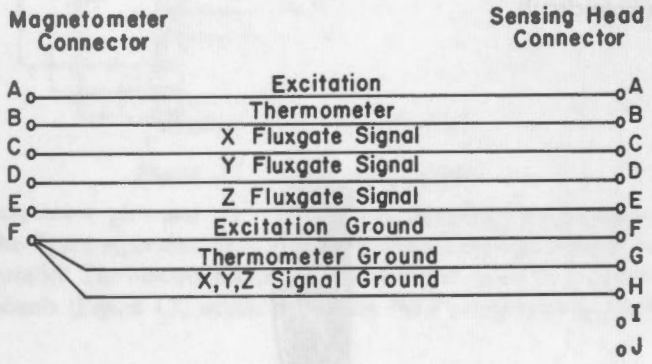

Figure 15. Cable wiring schematic.

Sensing head alignment

Experience has shown that the magnetic axis of the fluxgates differs from the physical axis by approximately 30 minutes of arc. This apparent defect is used as the basis of the head alignment procedure. The head is mounted with the "vertical" axis roughly parallel to F. Baseline controls are set at zero and the head is rotated about its axis. The magnetometer output provides a recording usually containing a large sinusoidal component as well as a d.c. level in the X and Y channel outputs. Proper adjustment of the levelling screws will eliminate the sinusoidal component of X and Y. At this point the axis of rotation is parallel to F. The remaining d.c. offset in the X and Y traces is a measure of the component of F seen by these fluxgates. It is eliminated by rotating the X and Y sensors about their own cylindrical axes. The magnetic axes of these two fluxgates then lie in a plane perpendicular to the physical axis of rotation, which is the desired alignment.

The reason for performing this adjustment becomes apparent from an examination of Figure 16. A horizontal fluxgate has been aligned to be perpendicular to H, i.e. measuring D. If this fluxgate were now tilted slightly in a vertical plane (Figure 16a) by an error angle θ, it would sense an axial component equal to $Z\sin\theta$ in the direction shown. Now, to give an apparent indication of D, it must be rotated by angle ϕ in the horizontal plane (Figure 16b) until the error component $Z\sin\theta$ is cancelled by another component of approximately $H\sin\phi$. Therefore:

$$Z \sin\theta \simeq H \sin\phi$$

$$\text{and } \phi \simeq \frac{Z\,\theta}{H} \quad (\sin\alpha \simeq \alpha \text{ for small } \alpha).$$

The angle between true D and apparent D is just ϕ. At Ottawa, Z is about four times as large as H, and so an error angle θ of the fluxgate magnetic axis towards the vertical produces a horizontal error angle $\phi \simeq 4\theta$.

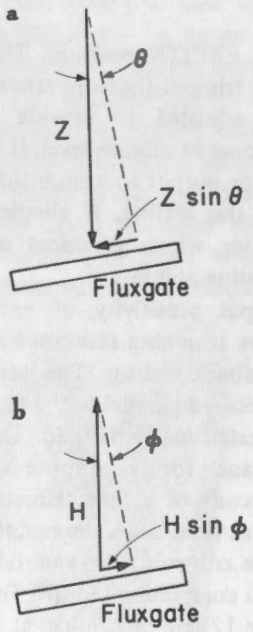

Figure 16.
(a) Error component sensed if the magnetic axis of a horizontal fluxgate sensor is tilted by an angle θ into a vertical plane
(b) Error angle ϕ necessary in the horizontal plane to compensate for the error component resulting from θ in the vertical plane.

Orientation of the head

Two head orientations are used extensively by the Earth Physics Branch. In these configurations the magnetometer measures the magnetic components D, H, Z or X, Y, Z. Orientation is relatively simple in the former case and this will be described first. To align in D, H and Z the head is levelled and the Y bias potentiometer is set to read zero. The meter switch on the magnetometer should be in the Y position. Rotation of the head about the vertical axis will bring the meter on scale and zero reading indicates the correct position or a position 180° from the correct one. Any one of three clues can be used to decide which of the two positions has been reached.

1. The pointer on the head will point to magnetic north in the correct orientation.
2. Clockwise rotation of the sensing head will result in clockwise rotation of the meter needle at the proper setting.
3. Incorrect setting makes it impossible to bring the X channel on scale with the X bias potentiometer (and meter switch at X).

If the wrong setting was obtained the head must be rotated 180 degrees and realigned. After this procedure the level should be re-checked. The X and Z channels may now be brought on scale using the bias potentiometers, and the X channel records magnetic H, the Y channel magnetic D and the Z channel magnetic Z. Several hours of recording will show whether or not the orientation procedure was performed during magnetic storm conditions. If it was, it should be repeated at a time when the traces are quiet.

In the auroral zone and further north the value of D at the time of orientation is too uncertain to permit use of the previous method. The head must then be oriented in geographical co-ordinates as determined by the position of the sun at local noon, the position of the pole star or a local survey. In those regions where the declination is east of true north, the pointer on the sensing head must point to true north. The X channel then records magnetic X, the Y channel magnetic Y and the Z channel magnetic Z. All channels can be brought on scale by using the bias potentiometers. In regions where the declination is west of true north the pointer on the sensing heads must point to true west. In this case, the X channel is used to record the Y component of the magnetic field and the Y channel is used to record the X field component.

Occasionally it is extremely difficult or impossible to determine geographical co-ordinates directly, and the following procedure may be attempted. Obtain estimated values of the magnetic components X and Y from magnetic maps or previous survey information in the area. Set the X and Y bias potentiometers to these estimated values using the bias field vs. potentiometer setting graph in Figure 7. Rotate the sensing head until the X and Y outputs come on scale. If they do not pass through zero simultaneously, increase or decrease the settings of both potentiometers by amounts proportional to their readings and repeat the procedure.

Troubleshooting

Waveforms which may be observed at eight points in the magnetometer circuit during correct operation are presented in Table II. The oscillator output (1) is taken at the output pin of the type 1520 power booster and should be a very clean sinusoidal wave of about 330 Hz frequency. Any distortion of the wave at this point means that the magnetometer is operating incorrectly and the output voltages do not accurately represent the magnetic field sensed by the associated sensor. Waveform (2) should appear at the junction of the 82-ohm resistor and the fluxgate primary winding. Although this wave looks very distorted, all even harmonics of 330 Hz are absent and so the sensor secondary windings pick up no even harmonics from the drive circuit. If there is an open circuit anywhere after the 82-ohm resistor, in either the cable or the fluxgate primaries, the wave at this point will be identical with (1).

The reference wave is generated by the full-wave rectifier consisting of the 143H transformer and 1N457 diodes. The wave (3) should appear at the junction of these 1N457 diodes and this is then amplified and filtered to give waveform (4) at the doubler output pin. This latter wave has a frequency of about 660 Hz. Once again, the magnetometer output cannot be relied upon if distortion is present at this point.

When a fluxgate sensor is operated in the null condition (zero axial magnetic field) waveform 5 will be present across the secondary winding. The only point to note here is that all even harmonics should be absent and whatever is left is noise. Examination of waveform (5) will reveal that the noise is primarily fundamental and third-harmonic fed over from the drive circuit, and this noise limits the gain available from the signal amplifier before wave-clipping occurs. The signal amplifier output (7) is just wave (5) amplified and filtered. Although the signal amplifier has maximum gain at the second-harmonic frequency (660 Hz), wave (7) should still contain only odd harmonics of 330 Hz at the null condition.

Waveform (6) illustrates the change that occurs as large axial magnetic field is applied to the sensor. This wave is also taken from the fluxgate secondary winding. The axial field is so large that the dynamic feedback is unable to cancel it and so second-harmonic voltage appears at the fluxgate secondary. After passing through the signal amplifier, where all harmonics are attenuated relative to 660 Hz the wave (8) appears at the amplifier output . Waves (6) and (8) have a high proportion of even-harmonic content.

References

Harrison, H.L. and J.G. Bollinger. 1963. Introduction to automatic controls, Chap. 6, 7, 9, *International Textbook Company*.

Primdahl, F. 1970. The fluxgate mechanism, *IEEE transactions on magnetics*, Vol. MAG-6, No. 2, 376.

Primdahl, F. 1970. A ferrite core fluxgate magnetometer, *Pub. Earth Physics Branch*, Vol. 40, No. 1.

Roy, J.L., W.A. Robertson and C. Keeping. 1969. Magnetic "field free" spaces for paleomagnetism, rock magnetism, and other studies. *Can. J. Earth Sci.*, 6, 1312.

Serson, P.H. 1957. An electrical recording magnetometer, *Can. J. Phys.*, 35, 1387.

Serson, P.H. and W.L.W. Hannaford. 1956. A portable electrical magnetometer, *Can. J. Tech.*, 34, 232.

Table II
Typical Waveforms

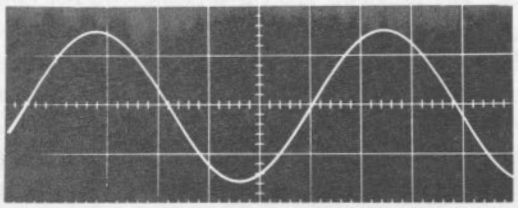

1. Oscillator Output
Hor: 0.5 ms/cm Vert: 5 v/cm

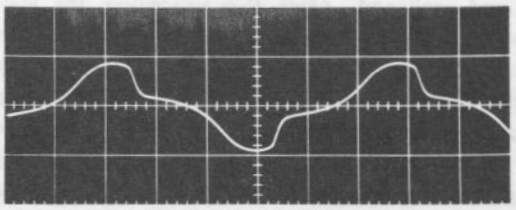

2. Fluxgate Primaries
Hor: 0.5 ms/cm Vert: 5 v/cm

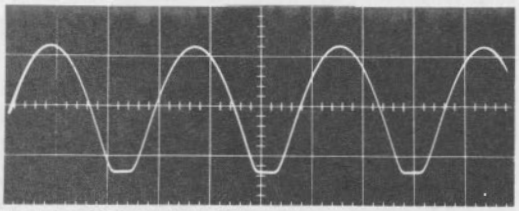

3. Rectifier Output
Hor: 0.5 ms/cm Vert: 0.5 v/cm

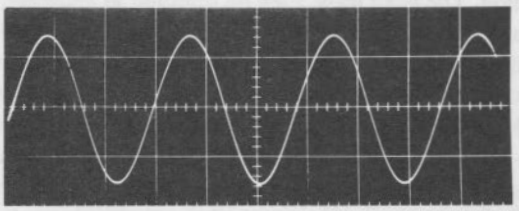

4. Doubler Output
Hor: 0.5 ms/cm Vert: 5 v/cm

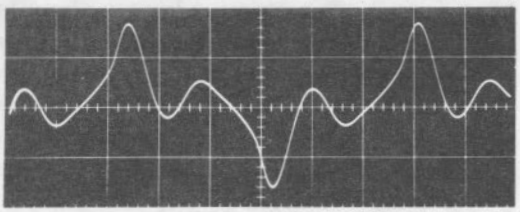

5. Fluxgate Secondary (at null)
Hor: 0.5 ms/cm Vert: 0.2 v/cm

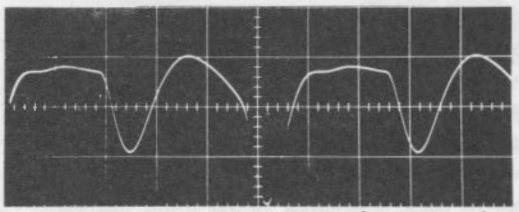

6. Fluxgate Secondary (off null)
Hor: 0.5 ms/cm Vert: 0.5 v/cm

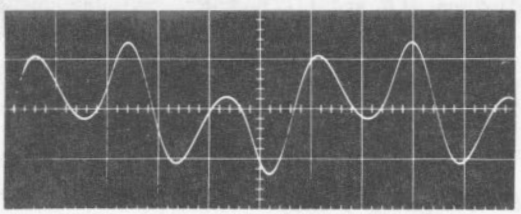

7. Amplifier Output (at null)
Hor: 0.5 ms/cm Vert: 2 v/cm

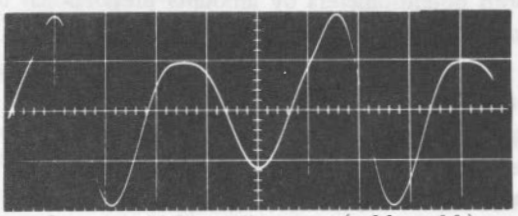

8. Amplifier Output (off null)
Hor: 0.5 ms/cm Vert: 5 v/cm

Appendix A – Calculation of frequency response

Substitute expressions for ω_n and δ into equation (1) to give:

$$\frac{s^2}{\omega_n^2} e_3 + \frac{2\delta}{\omega_n} s e_3 + e_3 = \frac{R_4}{A}\left(H_a - \frac{e_4 A}{R_5}\right)$$

or rearranging:

$$\frac{e_3}{H_a - \frac{e_4 A}{R_5}} = \frac{R_4}{A} \cdot \frac{1}{\left(\frac{s}{\omega_n}\right)^2 + 2\delta\left(\frac{s}{\omega_n}\right) + 1} = \frac{\text{output O(s)}}{\text{input I(s)}}$$

Substituting $s = j\omega$ gives:

$$\frac{O(j\omega)}{I(j\omega)} = \frac{R_4}{A} \cdot \frac{1}{\left(\frac{j\omega}{\omega_n}\right)^2 + 2\delta\left(\frac{j\omega}{\omega_n}\right) + 1}$$

$$= \frac{R_4}{A} \cdot \frac{1}{1 - \left(\frac{\omega}{\omega_n}\right)^2 + j2\delta\left(\frac{\omega}{\omega_n}\right)}$$

Multiplying numerator and denominator by conjugate of denominator:

$$\frac{O(j\omega)}{I(j\omega)} = \frac{R_4}{A} \cdot \left[\frac{1 - \left(\frac{\omega}{\omega_n}\right)^2 - j2\delta\left(\frac{\omega}{\omega_n}\right)}{\left[1 - \left(\frac{\omega}{\omega_n}\right)^2 + j2\delta\left(\frac{\omega}{\omega_n}\right)\right]\left[1 - \left(\frac{\omega}{\omega_n}\right)^2 - j2\delta\left(\frac{\omega}{\omega_n}\right)\right]}\right]$$

$$= \frac{R_4}{A} \cdot \frac{1 - \left(\frac{\omega}{\omega_n}\right)^2 - j2\delta\left(\frac{\omega}{\omega_n}\right)}{\left(\frac{\omega}{\omega_n}\right)^4 + (4\delta^2 - 2)\left(\frac{\omega}{\omega_n}\right)^2 + 1}$$

Call denominator $D = \left(\frac{\omega}{\omega_n}\right)^4 + (4\delta^2 - 2)\left(\frac{\omega}{\omega_n}\right)^2 + 1$

and let $X = 1 - \left(\frac{\omega}{\omega_n}\right)^2$ and $Y = -2\delta\left(\frac{\omega}{\omega_n}\right)$

Then $\frac{O(j\omega)}{I(j\omega)} = \frac{R_4}{AD}[X + jY]$

The magnitude $M(\omega)$ of $\frac{O(j\omega)}{I(j\omega)}$ is equal to $\frac{R_4 (X^2+Y^2)^{\frac{1}{2}}}{AD}$

Observe that $D = X^2 + Y^2$

Therefore $M(\omega) = \frac{R_4 D^{\frac{1}{2}}}{AD} = \frac{R_4 D^{-\frac{1}{2}}}{A}$

$$M(\omega) = \frac{R_4}{A}\left[\left(\frac{\omega}{\omega_n}\right)^4 + (4\delta^2 - 2)\left(\frac{\omega}{\omega_n}\right)^2 + 1\right]^{-\frac{1}{2}}$$

The phase angle $\phi(\omega)$ between $O(j\omega)$ and $I(j\omega)$ is $\phi(\omega) = \cos^{-1}[X(X^2+Y^2)^{-\frac{1}{2}}] = \cos^{-1}(XD^{-\frac{1}{2}})$

$$\phi(\omega) = \cos^{-1}\left\{\left[1 - \left(\frac{\omega}{\omega_n}\right)^2\right]\left[\left(\frac{\omega}{\omega_n}\right)^4 + (4\delta^2 - 2)\left(\frac{\omega}{\omega_n}\right)^2 + 1\right]^{-\frac{1}{2}}\right\}$$

Appendix B – Temperature compensation

The following equations are obtained from examination of Figure 17:

$$e_1 = e_0 - e_z - i_z R_z$$

and $e_1 = i_z R_1$

Eliminating i_z:

$$e_1 = \frac{R_1}{R_1 + R_z}(e_0 - e_z)$$

Also,

$$e_2 = \frac{R_3 + R_4}{R_2 + R_3 + R_4} e_0$$

where R_4 is the sum of the 100-ohm platinum resistance plus 3 ohms allowed for a 250-ft sensing head cable of #18 wire. Temperature coefficient is assumed to be +3900 ppm/°C in both cases.

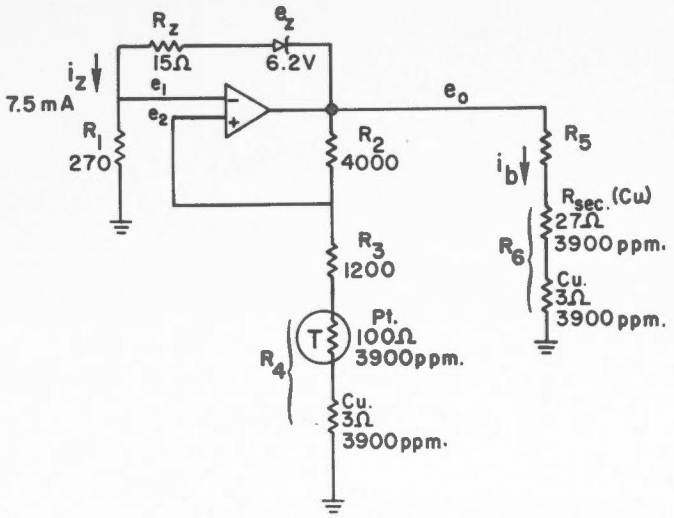

Figure 17. Schematic of the temperature compensation network.

Because of the action of the operational amplifier, $e_1 = e_2$

$$\therefore e_o = \frac{e_z}{1 - \frac{(R_3+R_4)(R_1+R_z)}{R_1(R_2+R_3+R_4)}}$$

At O°C: $e_z = 6.2V$, $R_1 = 270\Omega$, $R_2 = 4000\Omega$, $R_3 = 1200\Omega$
$R_4 = 103\Omega$
$e_o = 8.37114$ V
At 25°C: $e_z = 6.2V$, $R_1 = 270\Omega$, $R_2 = 4000\Omega$, $R_3 = 1200\Omega$,
$R_4 = 113\Omega$
$e_o = 8.38812$ V.

$$\frac{\Delta e_o}{e_o \Delta T} = \frac{+0.01698\ V}{8.37 \times 25} = +81\ \text{ppm/°C}$$

Consequently, reference voltage increases at a rate of 81 ppm/°C.
Bias current i_b is determined by total resistance $R_5 + R_6$,
and if Z=60,000γ:

$$R_5+R_6 = \frac{8.37V \times 340\ oe}{0.60\ oe \quad A} = 4740\Omega$$

and $R_5 = 4740\Omega - 30\Omega = 4710\Omega$

Temperature changes in bias current from the effect of R_6 will be:

$$\frac{\Delta i_b}{i_b} = \frac{-\Delta R_6}{R_6} \times \frac{R_6}{(R_5+R_6)}$$

$$\therefore \frac{\Delta i_b}{i_b} = -25\ \text{ppm/°C}$$

with the minus sign indicating a decrease in bias current with an increase in temperature (and resistance). The net temperature effect is then the sum of bias voltage coefficient and bias current coefficient due to changes in R_6.

$$\text{Net}\frac{\Delta i_b}{i_b} = 81 - 25 = 56\ \text{ppm/°C}$$